July 15, 1999 CB-note 345

Technical Report:

$\bar{p}p$ annihilation at rest into two-body final states and branching ratios (GH_2)

Burkhard Pick

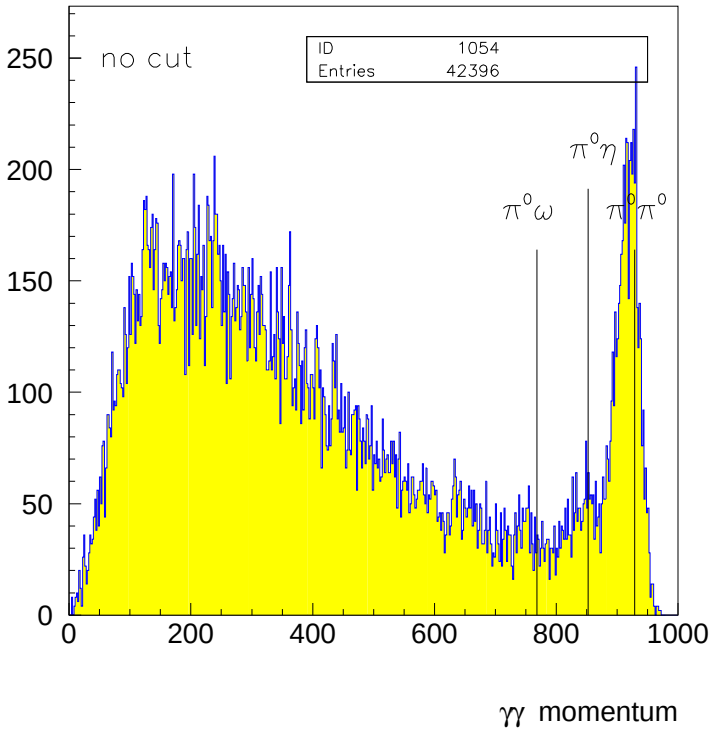

Institut für Strahlen– und Kernphysik, Universität Bonn, D–53115 Bonn

http://www.iskp.uni-bonn.de/cbiskp/cbiskp.html

Contents

Chapter 1

Introduction

This report gives a survey of two-body $\bar{p}p$ branching ratios in gaseous hydrogen. The target pressure amounts to 12 atm

All steps of the analysis are technically oriented at the method introduced in report [1] dealing with the branching ratios in liquid hydrogen. Therefore here all things written in the former report are not repeated.

1.1 The July 1996 minimum bias data

The data analysis discussed in this report is based on the runs (GH_2 target) listed below. The trigger file was called `minbias.default`.

37510 GK0457	37739 GK0463	38035 GK0469	38178 GK0473
37511 GK0457	37740 GK0463	38036 GK0469	38179 GK0473
37515 GK0457	37775 GK0464	38056 GK0469	38218 GK0474
37516 GK0457	37776 GK0464	38057 GK0469	38219 GK0474
37517 GK0457	37777 GK0464	38081 GK0470	38220 GK0474
37529 GK0457	37826 GK0465	38083 GK0470	38221 GK0474
37591 GK0459	37827 GK0465	38084 GK0470	38251 GK0476
37592 GK0459	37828 GK0465	38085 GK0470	38252 GK0476
37601 GK0459	37829 GK0465	38120 GK0471	38253 GK0476
37602 GK0459	37870 GK0466	38121 GK0471	38274 GK0476
37603 GK0459	37872 GK0466	38122 GK0471	38275 GK0476
37604 GK0459	37879 GK0466	38146 GK0472	38317 GK0478
37605 GK0459	37942 GK0467	38147 GK0472	38318 GK0478
37682 GK0461	37943 GK0467	38148 GK0472	38320 GK0478
37683 GK0461	37997 GK0468	38149 GK0472	38368 GK0479
37685 GK0461	37998 GK0468	38174 GK0473	38397 GK0480
37712 GK0462	37999 GK0468	38175 GK0473	
37737 GK0462	38000 GK0468	38176 GK0473	
37738 GK0463	38034 GK0469	38177 GK0473	

The total number of physical events is 2 656 240. After pile-up cut 2 593 580 events.

1.2 Annihilation outside the target

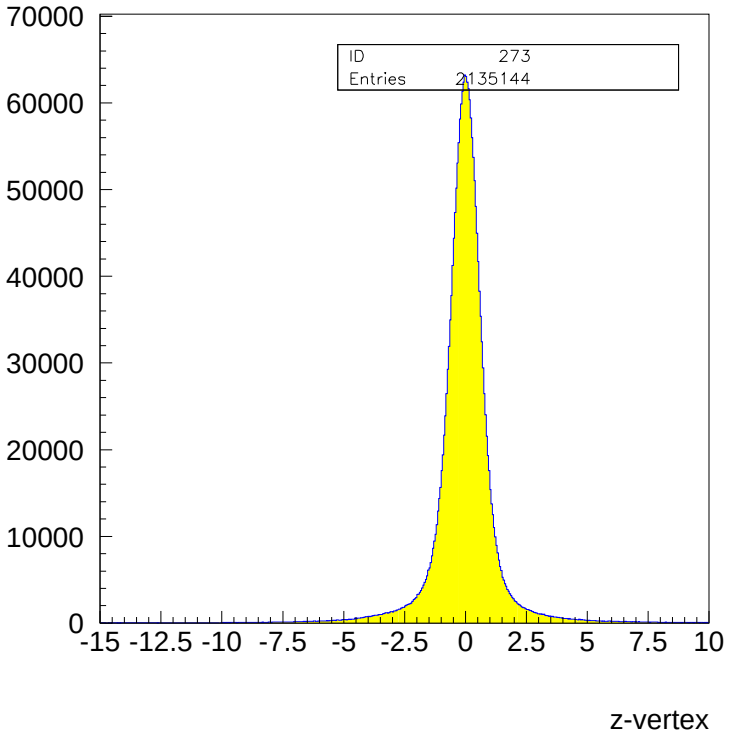

Figure 1.1: Vertex z distribution for charged tracks.

Figure 1.1 shows that there are no annihilations outside the target.

1.3 The Monte Carlo data

All Monte Carlo events are produced in the same way as for liquid hydrogen. Table 1.1 summarizes this.

final state	CBGEANT particle id	number of events
$\pi^0\pi^0$	7, 7	582 476
$\pi^0\eta$	7, 62	592 153
$(K_S \to \pi^0\pi^0)K_L^{missing}$		573 507
$\pi^+\pi^-$	8, 9	600 000
K^+K^-	11, 12	600 000

Table 1.1: List of produced Monte Carlo data.

Chapter 2

4-γ events

Figure 2.1 shows the momenta and invariant masses of all six combinations from the July 1996 run (GH_2).

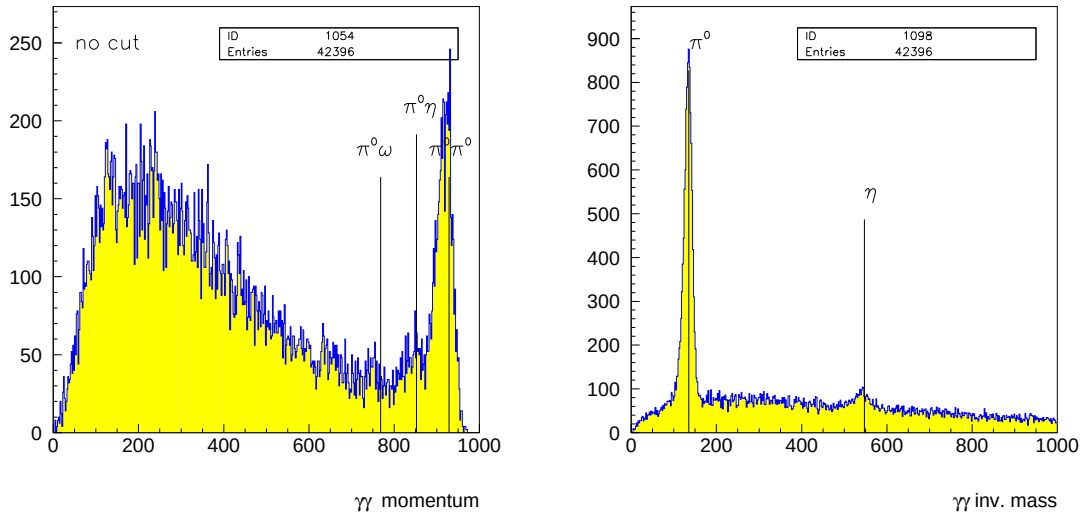

Figure 2.1: (left) Momentum of all six 2-γ combinations. Each $\pi^0\pi^0$ event causes two entries in the peak on the right side.
(right) Invariant mass of all six 2-γ combinations.

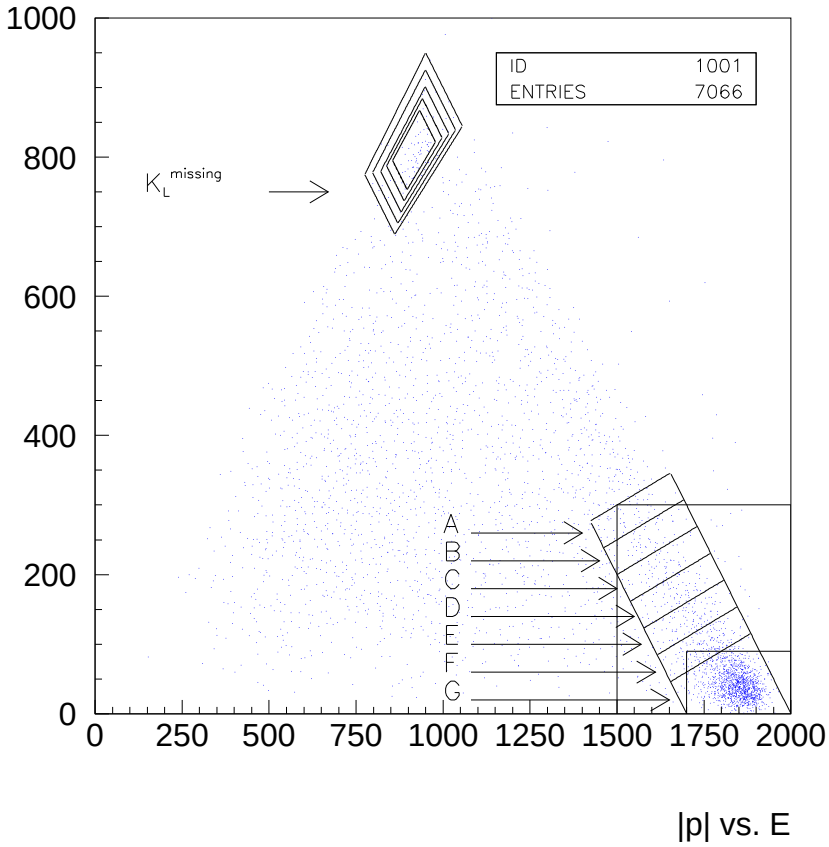

Figure 2.2: $|\vec{p}|$ vs. E. The kinematics for the marked areas are given in report [1].

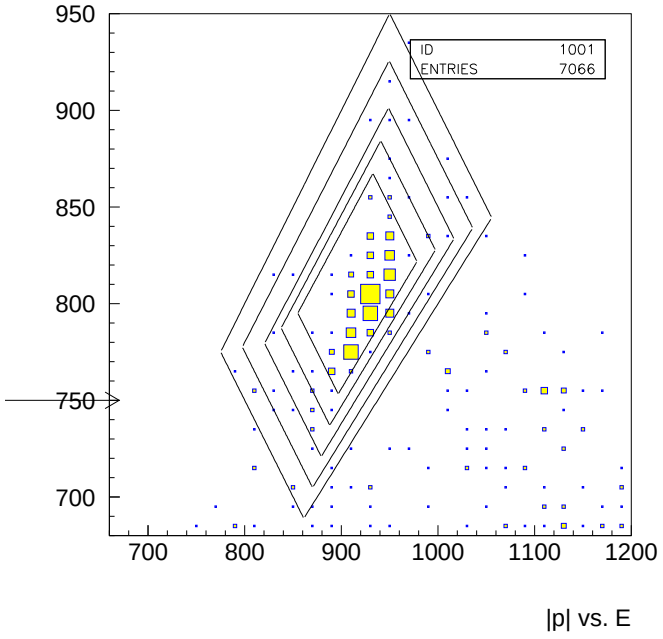

Figure 2.3: $|\vec{p}|$ vs. E. The same as in figure 2.2, but only the K_L-region is shown.

2.1 $\bar{p}p \to \pi^0\pi^0$ and $\pi^0\eta$

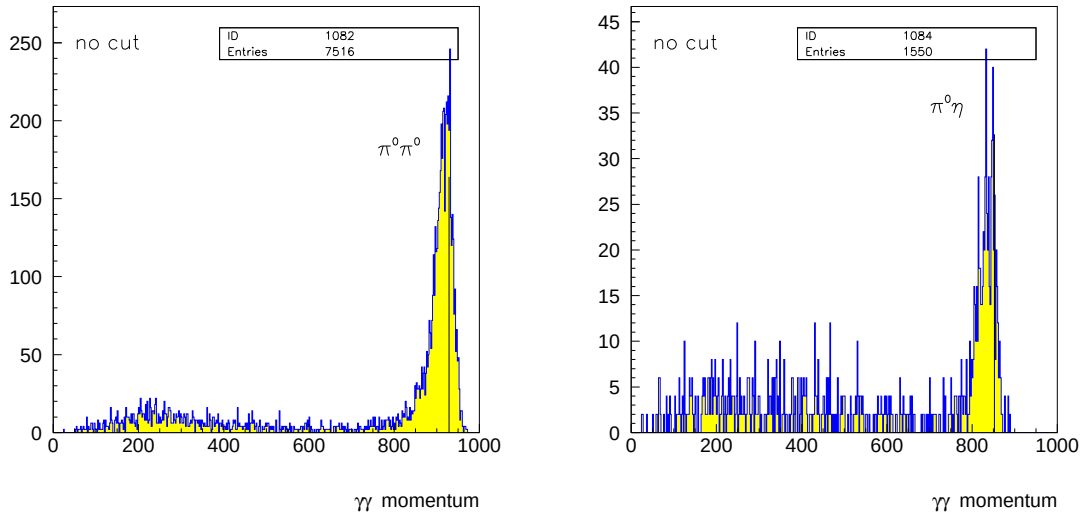

Figure 2.4: (left) Momentum of γ's for $\pi^0\pi^0$ final state.
(right) Momentum of η's for $\pi^0\eta$ final state.

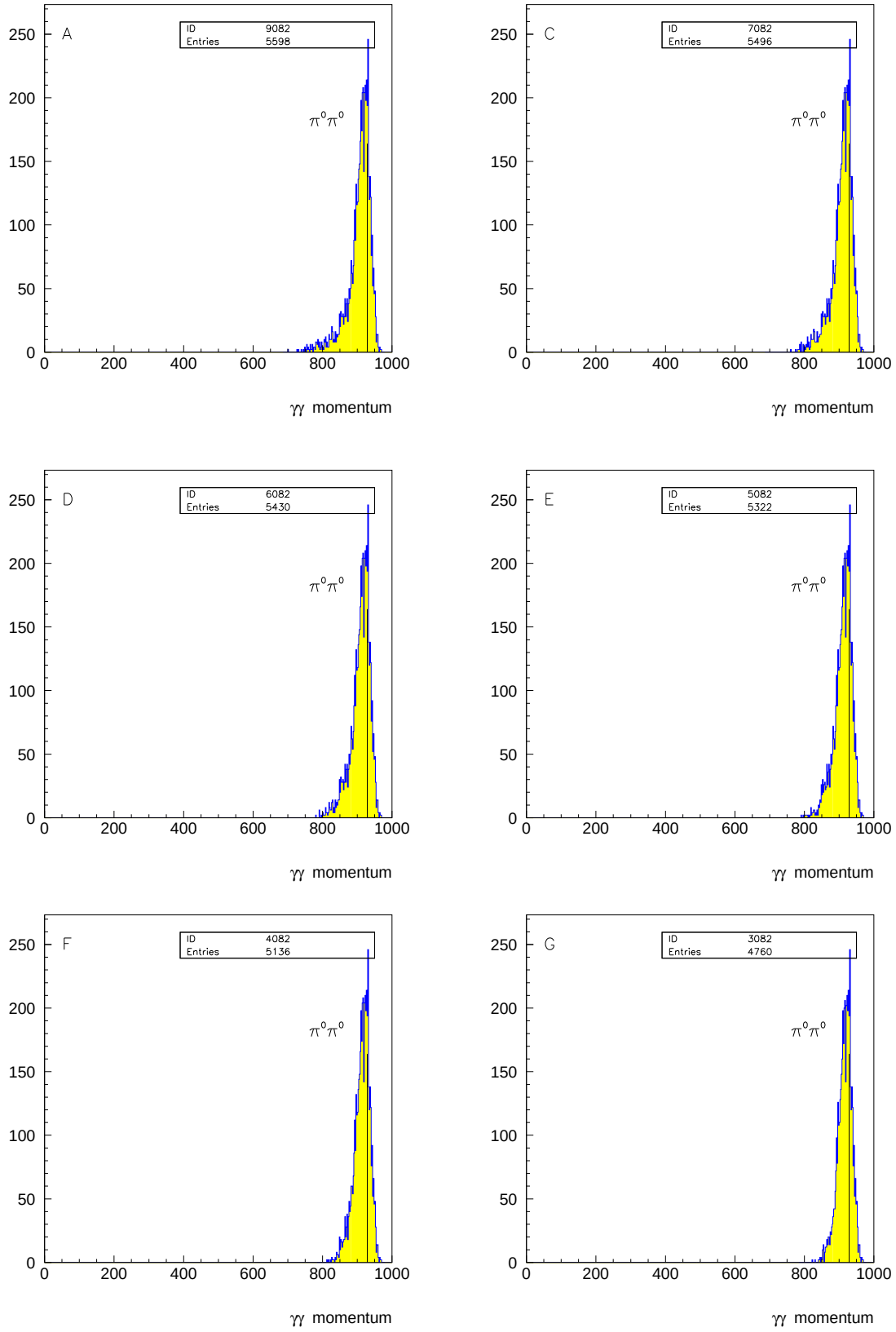

Figure 2.5: Momentum of π^0's for $\pi^0\pi^0$ final state. The letters are refering to the kinematical regions listed in report [1].

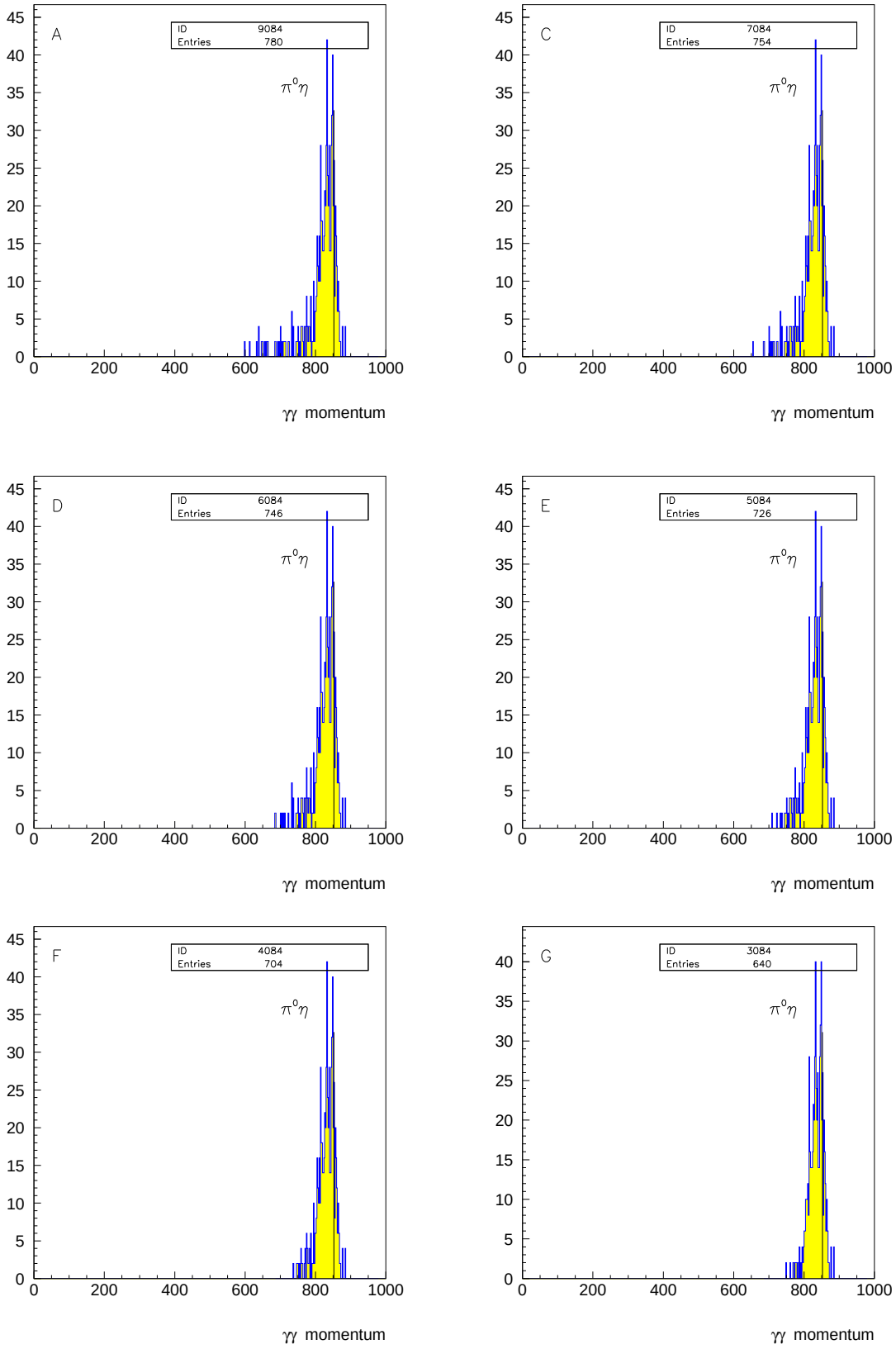

Figure 2.6: Momentum of π^0's and η's for $\pi^0\eta$ final state. The letters are refering to the kinematical regions listed in report [1].

2.2 $\bar{p}p \to K_L K_S$

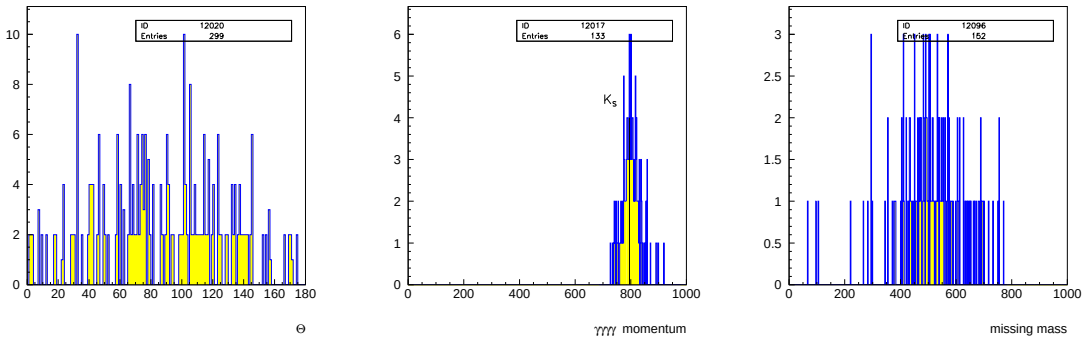

Figure 2.7: (left) Angular distribution for the measured momentum.
(center) Momentum of 2 γ's for $K_L K_S$ final state ($21° < \theta < 159°$)
(right) Missing mass of 2 γ's for $K_L K_S$ final state.

2.3 $\pi^0\pi^0$ Monte Carlo events

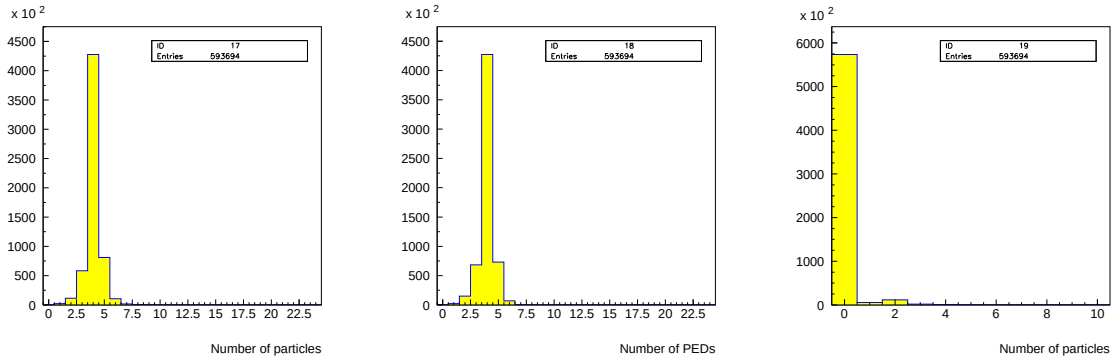

Figure 2.8: The number of particles, PEDs and charged tracks for 582 476 produced Monte Carlo events.

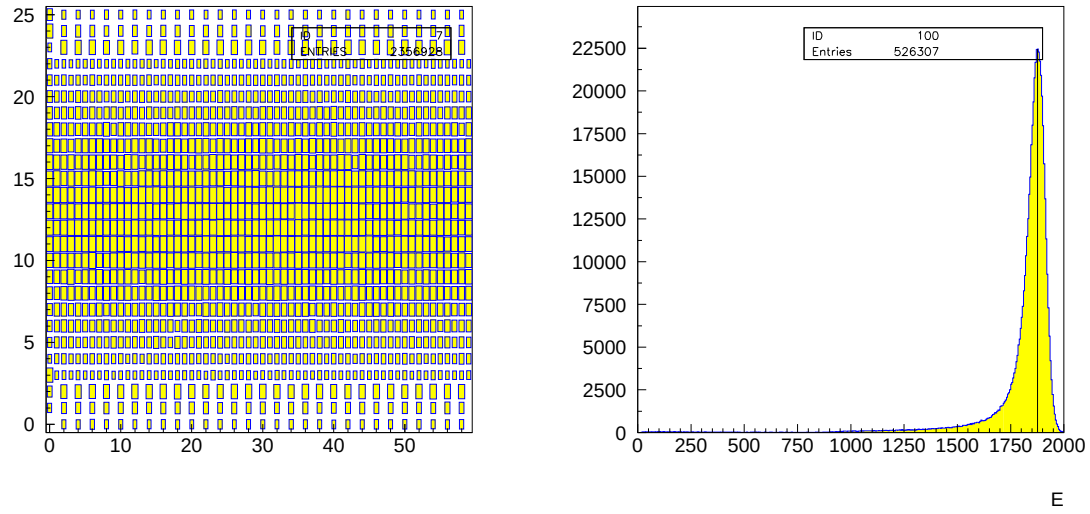

Figure 2.9: (left) Unfolded view of the calorimeter for Monte Carlo events.
(right) Energy of all γ's for Monte Carlo events.

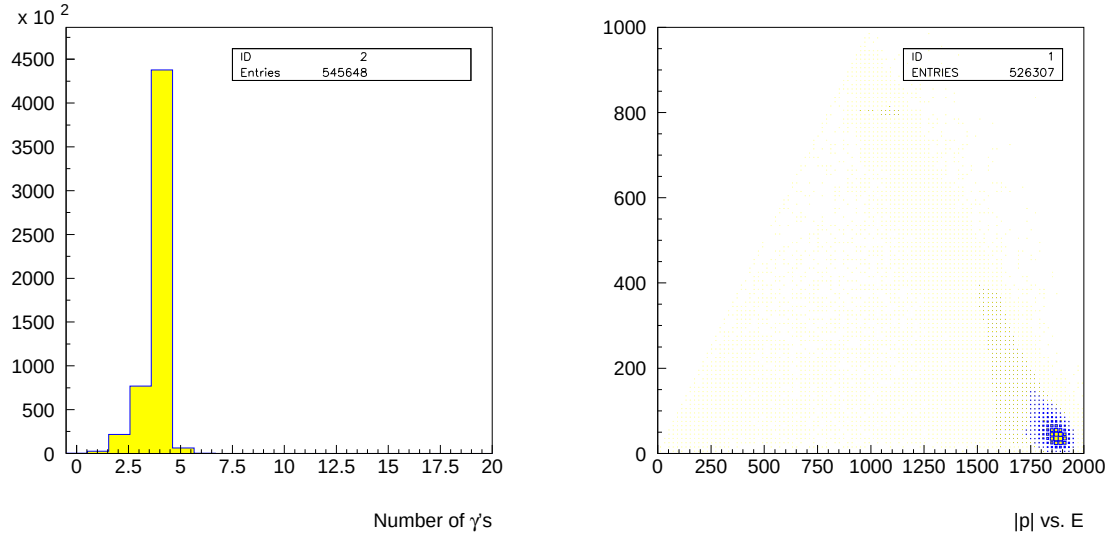

Figure 2.10: (left) γ distribution for Monte Carlo events.
(right) $|\vec{p}|$ vs. E for Monte Carlo events.

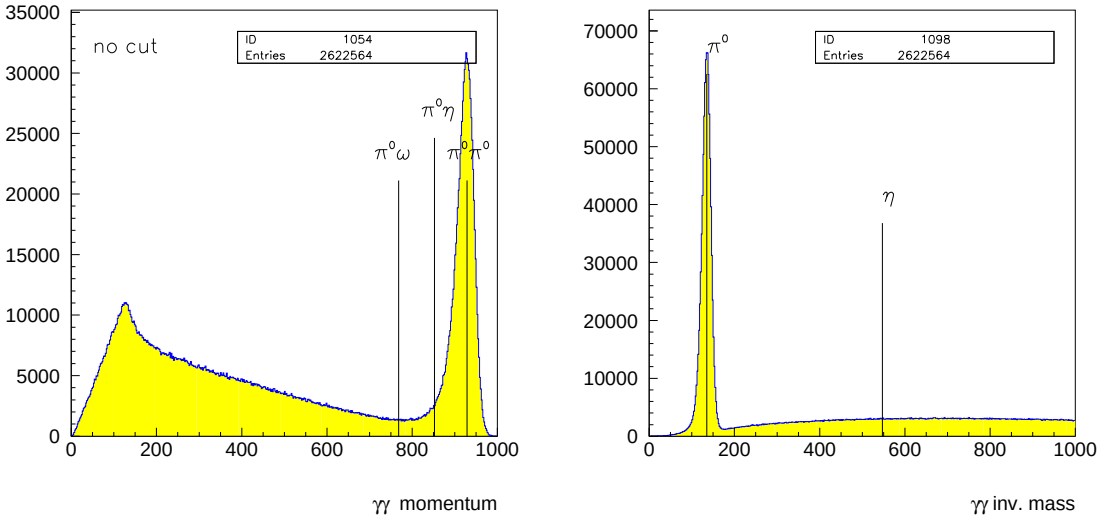

Figure 2.11: (left) Momentum of all 2 π^0's. Each $\pi^0\pi^0$ events causes two entries in the peak on the right side.
(right) Invariant masses of 2 γ's.

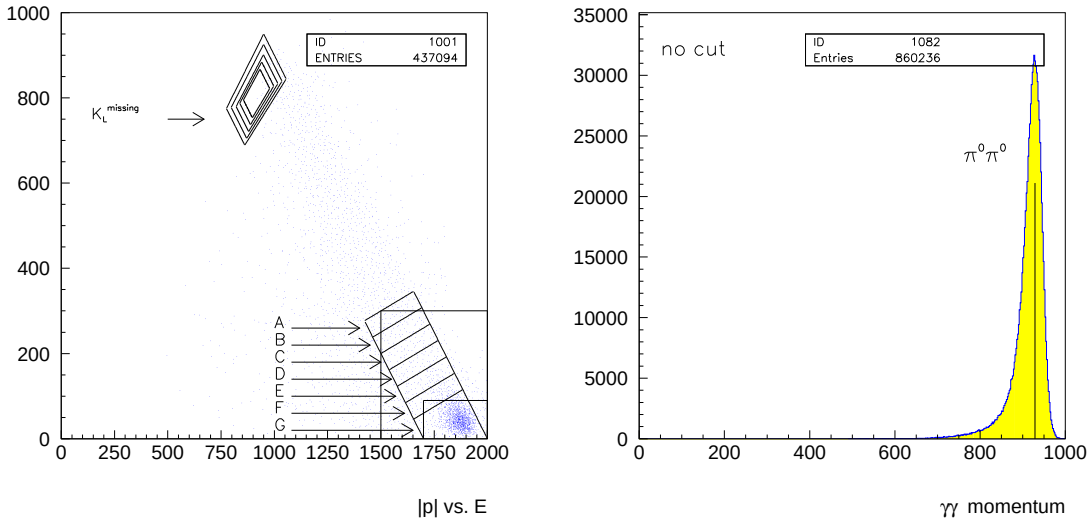

Figure 2.12: (left) $|\vec{p}|$ vs. E. The kinematics for the marked areas are given in report [1].
(right) Momentum of π^0's for $\pi^0\pi^0$ final state.

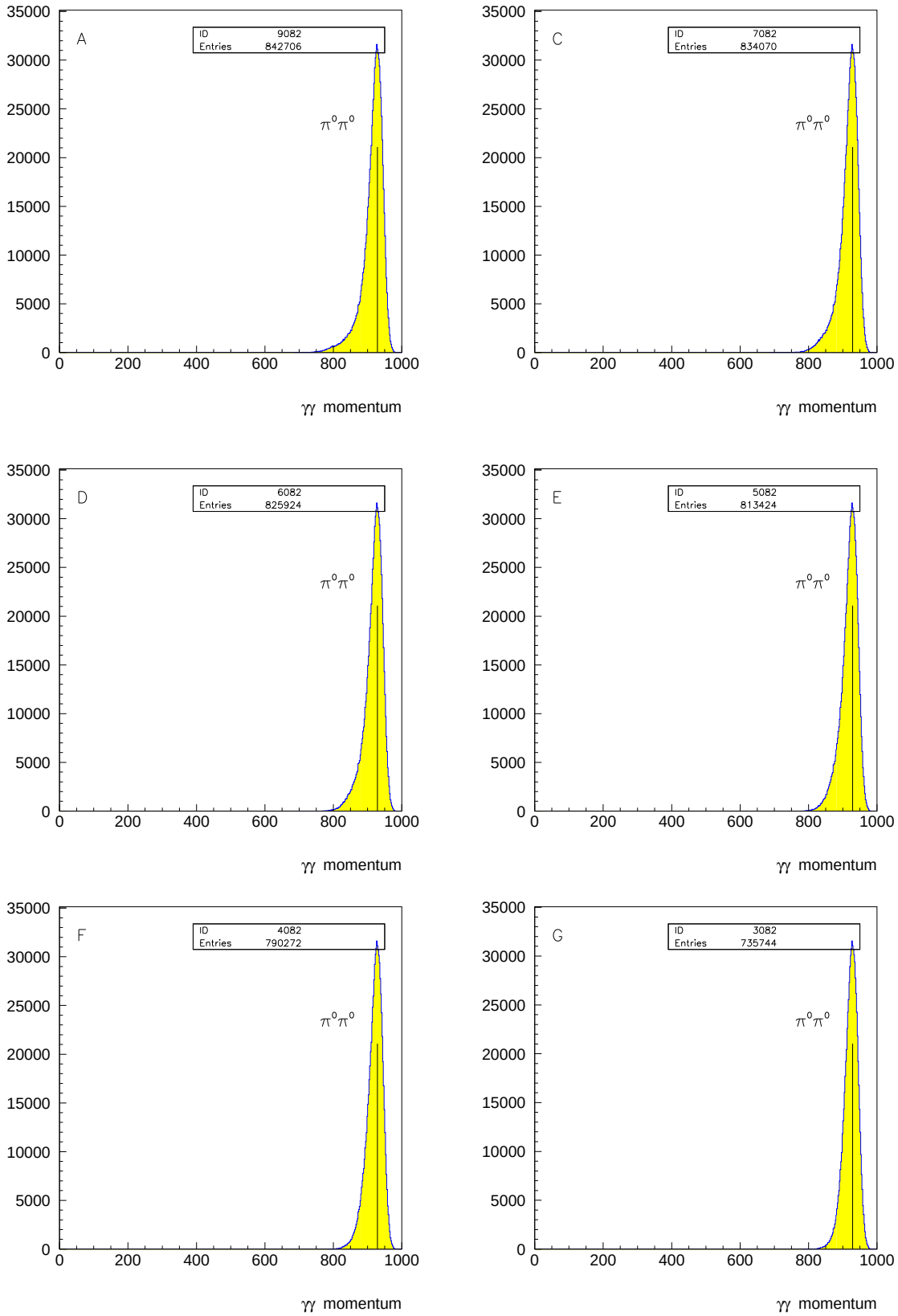

Figure 2.13: Momentum of π^0's for $\pi^0\pi^0$ final state. The letters are refering to the kinematical regions listed in report [1].

2.4 $\pi^0\eta$ Monte Carlo events

η's decaying with 100% into 2γ have been produced. This has to be corrected because a real η decays into 2γ only for $(39.25 \pm 0.31)\%$ [2].

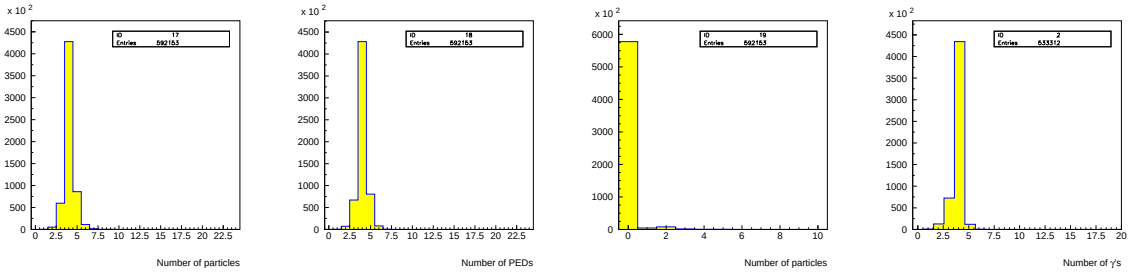

Figure 2.14: The number of particles, PEDs and charged tracks for 579 585 produced Monte Carlo events. γ distribution for Monte Carlo events.

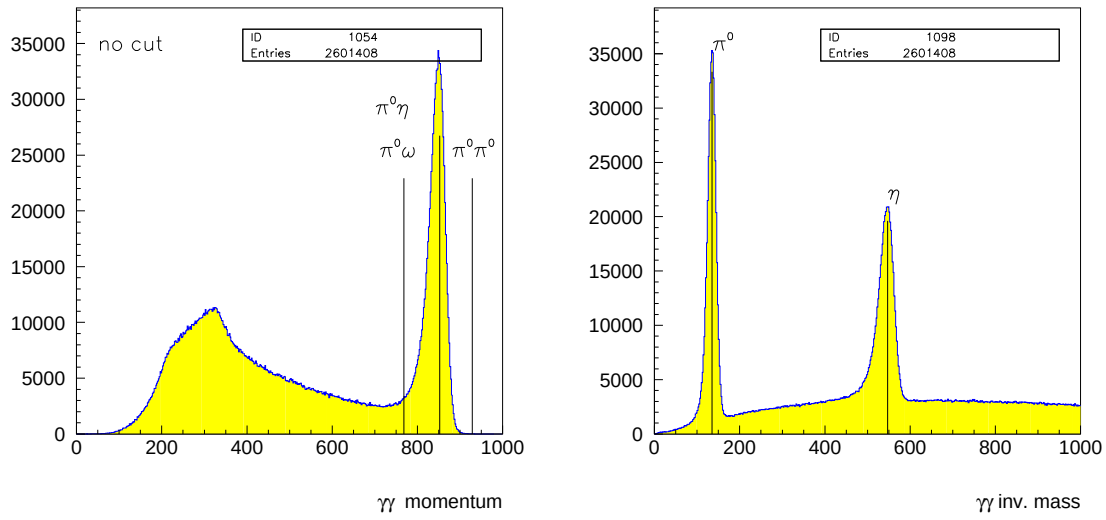

Figure 2.15: (left) Momentum of π^0's. Each $\pi^0\eta$ events causes two entries in the peak on the right side.
(right) Invariant masses of 2 γ's.

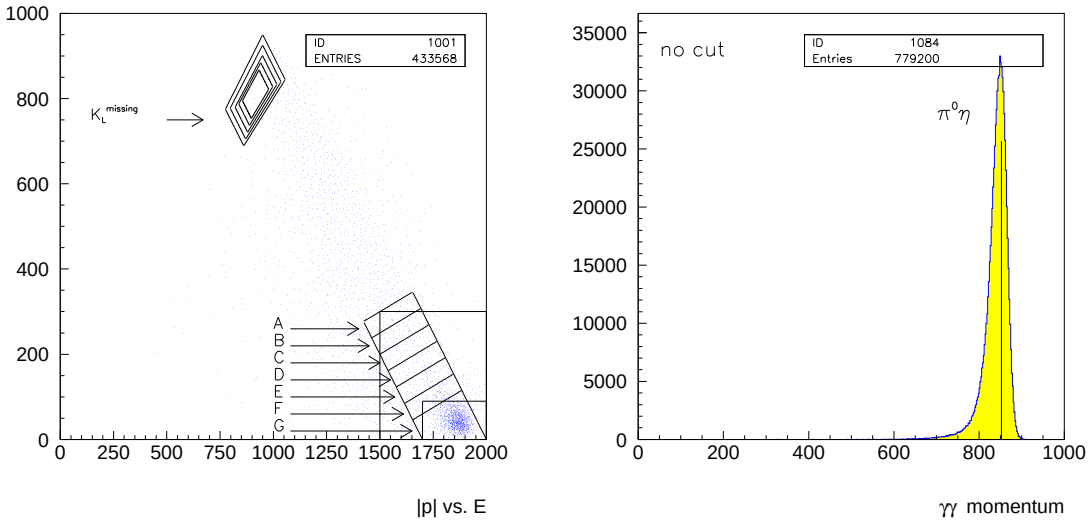

Figure 2.16: (left) $|\vec{p}|$ vs. E. The kinematics for the marked areas are given in report [1]. (right) Momentum of γ's for $\pi^0\eta$ final state.

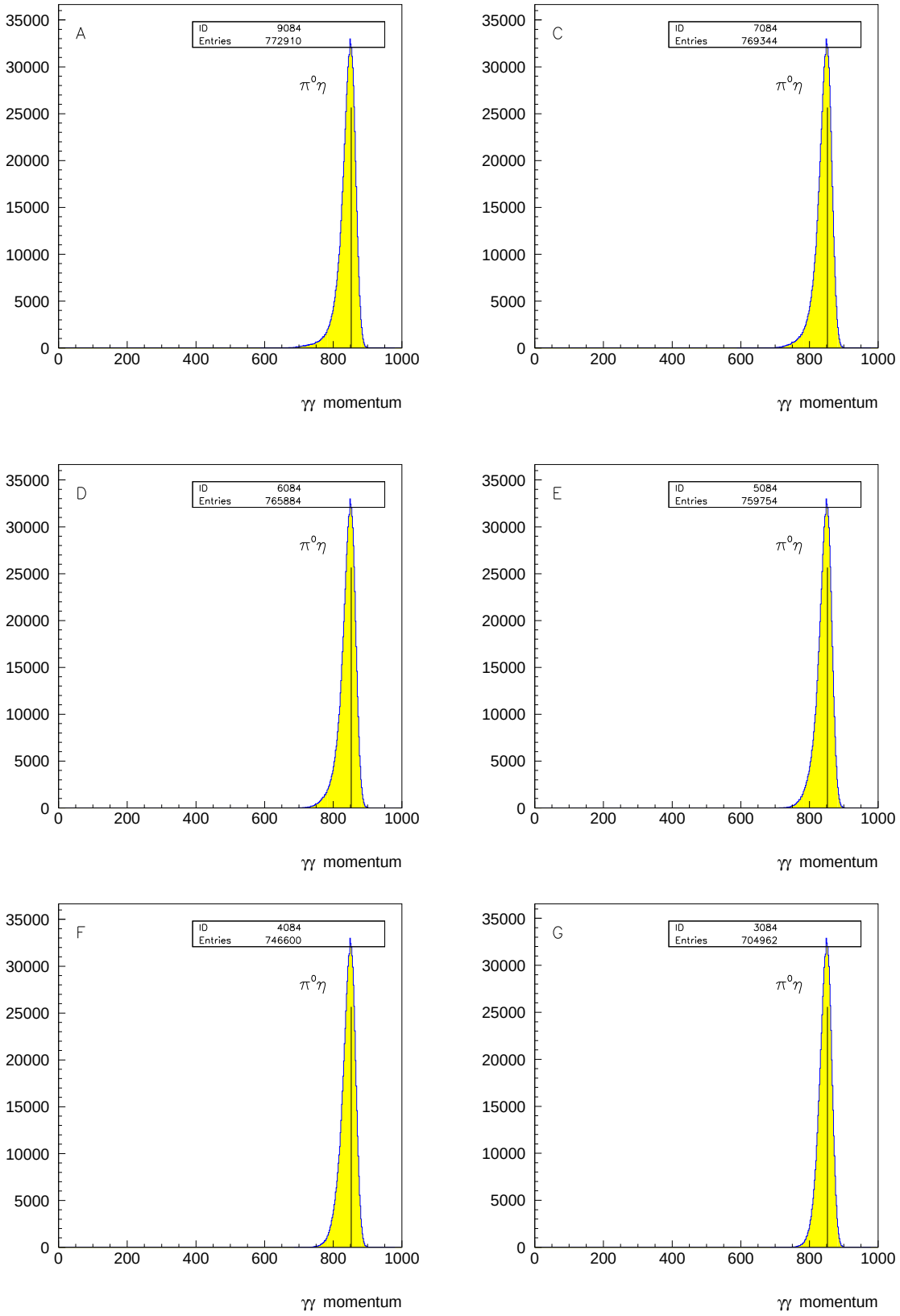

Figure 2.17: Momentum of π^0's and η's for $\pi^0\eta$ final state. The letters are refering to the kinematical regions listed in report [1].

2.5 $K_S K_L$ Monte Carlo events

The produced K_S decay with 100% into $\pi^0\pi^0$. The K_L decay into two noninteracting Monte Carlo particles, called geantinos. The very short decay time of $\tau = 10^{-20}$ sec ensures that there is no interaction between the K_L and the detector possible.

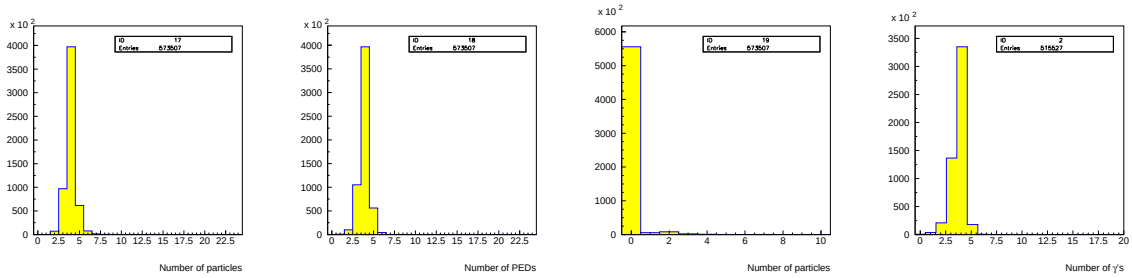

Figure 2.18: The number of particles, PEDs and charged tracks for 599 873 produced Monte Carlo events. γ distribution for Monte Carlo events.

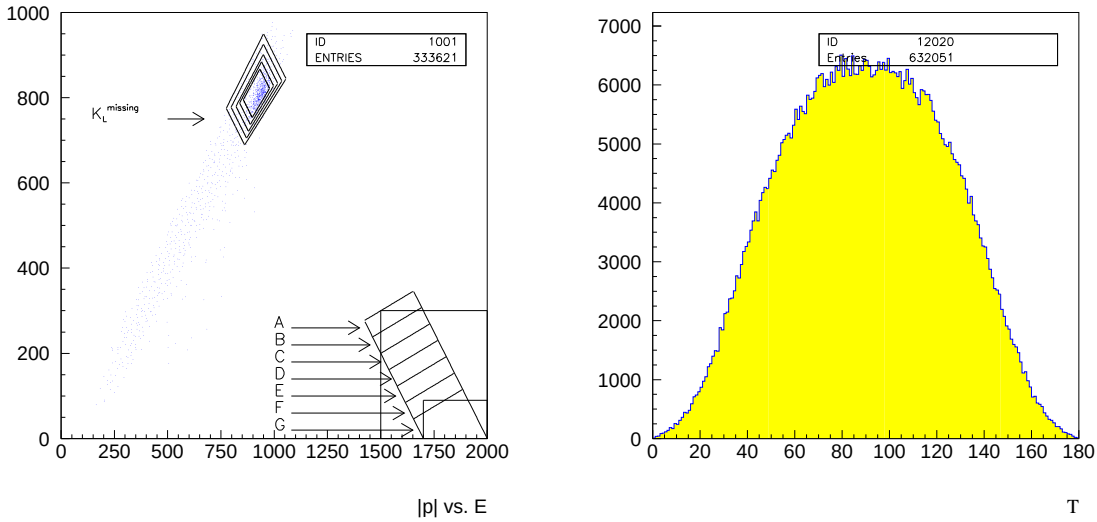

Figure 2.19: (left) $|\vec{p}|$ vs. E for Monte Carlo events.
(right) Angular distribution for measured momentum.

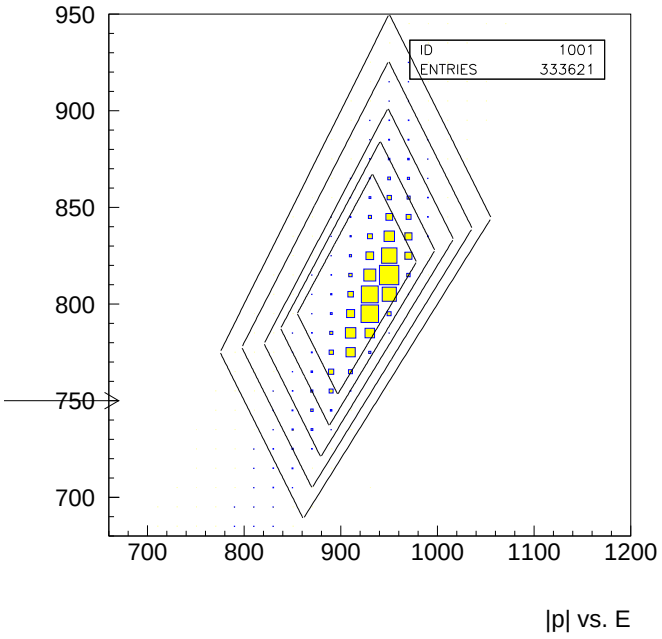

Figure 2.20: The same as in figure 2.19, but only the K_L-region is shown.

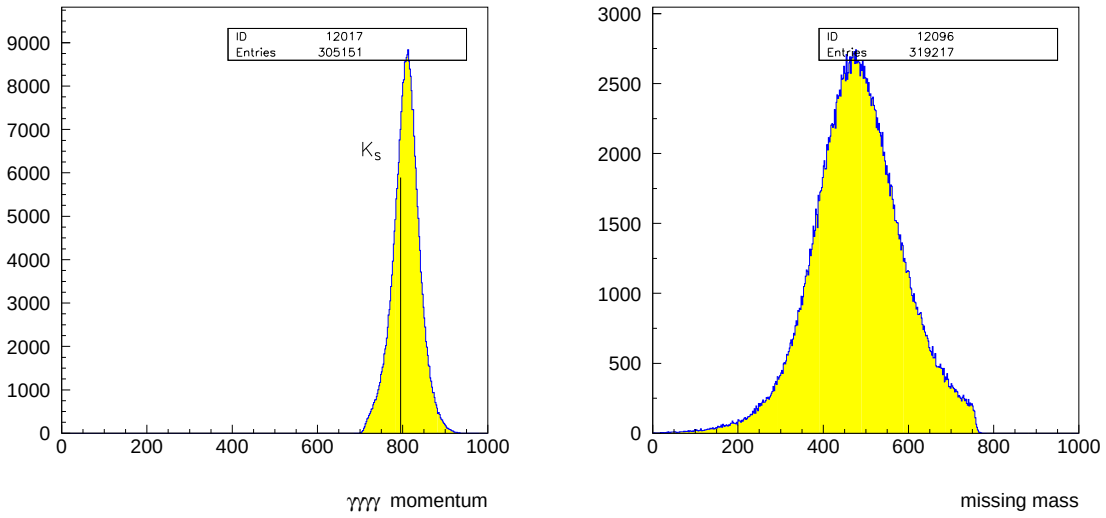

Figure 2.21: (left) Momentum of 2 γ's for $K_L K_S$ final state ($21° < \theta < 159°$).
(right) Missing mass of 2 γ's for $K_L K_S$ final state.

2.6 The Branching Ratios

The kinematical regions refer to [1].

region	#($\pi^0\pi^0$)	#(rec. MC)	$BR(\bar{p}p \to \pi^0\pi^0)$
A	2 799	421 353	$(1.521 \pm 0.081) \cdot 10^{-3}$
B	2 773	419 661	$(1.513 \pm 0.081) \cdot 10^{-3}$
C	2 748	417 035	$(1.508 \pm 0.081) \cdot 10^{-3}$
D	2 715	412 962	$(1.505 \pm 0.081) \cdot 10^{-3}$
E	2 661	406 712	$(1.498 \pm 0.080) \cdot 10^{-3}$
F	2 568	395 136	$(1.488 \pm 0.080) \cdot 10^{-3}$
G	2 380	367 872	$(1.481 \pm 0.080) \cdot 10^{-3}$
H	2 807	425 181	$(1.511 \pm 0.081) \cdot 10^{-3}$
I	2 390	364 877	$(1.499 \pm 0.081) \cdot 10^{-3}$

Table 2.1: $\pi^0\pi^0$ branching ratios.

region	#($\pi^0\eta$)	#(rec. MC)	$BR(\bar{p}p \to \pi^0\eta)$
A	390	386 455	$(5.870 \pm 0.418) \cdot 10^{-4}$
B	383	385 715	$(5.776 \pm 0.413) \cdot 10^{-4}$
C	377	384 672	$(5.701 \pm 0.409) \cdot 10^{-4}$
D	373	382 942	$(5.666 \pm 0.408) \cdot 10^{-4}$
E	363	379 877	$(5.559 \pm 0.403) \cdot 10^{-4}$
F	352	373 300	$(5.485 \pm 0.401) \cdot 10^{-4}$
G	320	352 481	$(5.281 \pm 0.396) \cdot 10^{-4}$
H	391	387 855	$(5.864 \pm 0.417) \cdot 10^{-4}$
I	329	350 079	$(5.467 \pm 0.407) \cdot 10^{-4}$

Table 2.2: $\pi^0\eta$ branching ratios.

region	#(K_LK_S)	#(rec. MC)	$BR(\bar{p}p \to K_LK_S)$
J	133	305 151	$(7.174 \pm 0.718) \cdot 10^{-4}$
K	130	301 560	$(7.095 \pm 0.716) \cdot 10^{-4}$
L	122	294 127	$(6.827 \pm 0.706) \cdot 10^{-4}$
M	113	277 886	$(6.693 \pm 0.713) \cdot 10^{-4}$
N	103	238 203	$(7.117 \pm 0.786) \cdot 10^{-4}$

Table 2.3: K_LK_S neutral branching ratios.

In order to determine the final values of the branching ratios the same kinematical regions as in [1] has been chosen. For $\pi^0\pi^0$ and $\eta\eta$ these are regions E and F and for K_LK_S this is region L.

$$BR(\bar{\mathrm{p}}\mathrm{p}(\mathrm{GH}_2) \to \pi^0\pi^0) = (1.49 \pm 0.08) \cdot 10^{-3} \tag{2.1}$$

$$BR(\bar{\mathrm{p}}\mathrm{p}(\mathrm{GH}_2) \to \pi^0\eta) = (5.52 \pm 0.40) \cdot 10^{-4} \tag{2.2}$$

$$BR(\bar{\mathrm{p}}\mathrm{p}(\mathrm{GH}_2) \to \mathrm{K_L K_S}) = (6.83 \pm 0.71) \cdot 10^{-4} \tag{2.3}$$

Chapter 3

2-prong events

From all events remaining after the preselection 2-prong events are selected.

Figure 3.1 shows the momenta of the two prongs from the July 1996 run (GH_2).

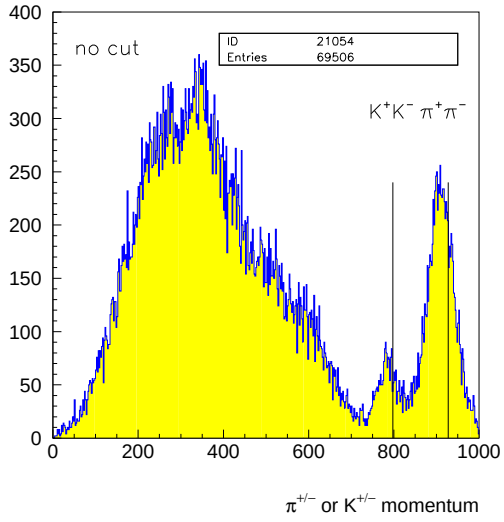

Figure 3.1: Momentum of two prongs. Each event causes two entry.

3.1 $\bar{p}p \to \pi^+\pi^-$ and K^+K^-

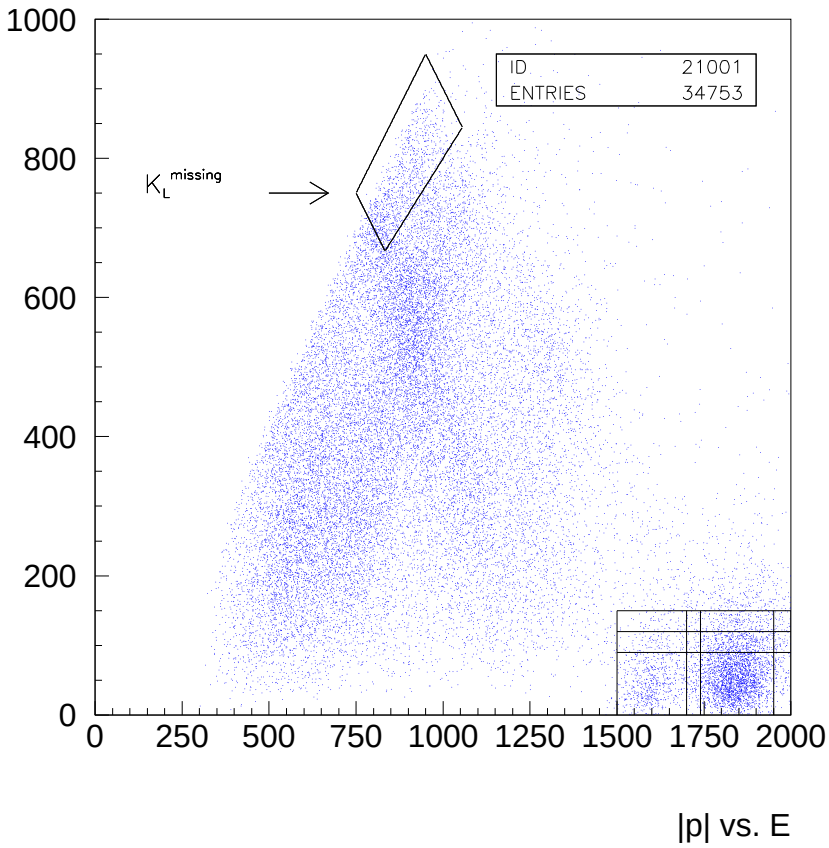

Figure 3.2: $|\vec{p}|$ vs. E for 2-prong data.

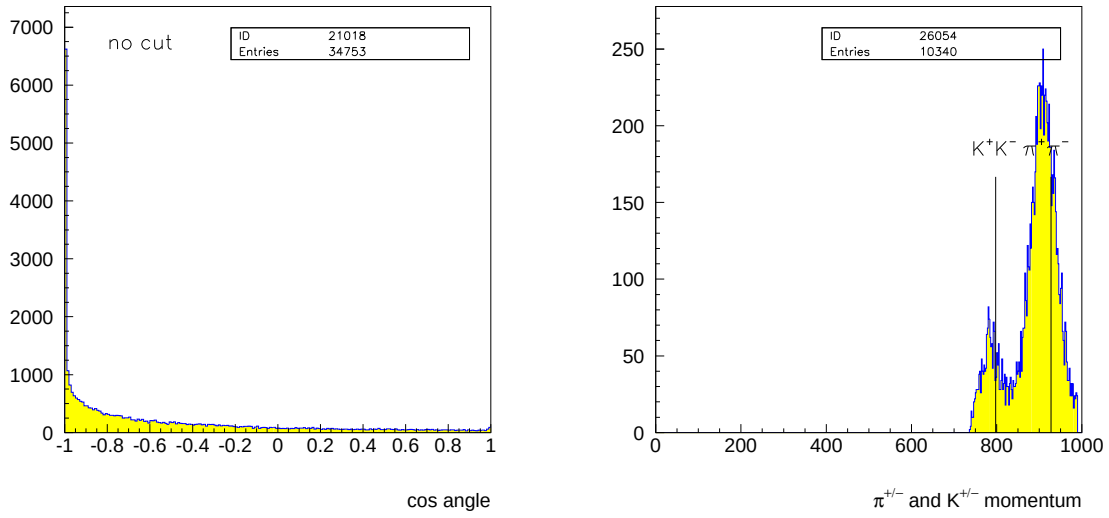

Figure 3.3: (left) cos of the angle between the two tracks.
(right) Momentum of two prongs. Each event causes two entry (regions A and B).

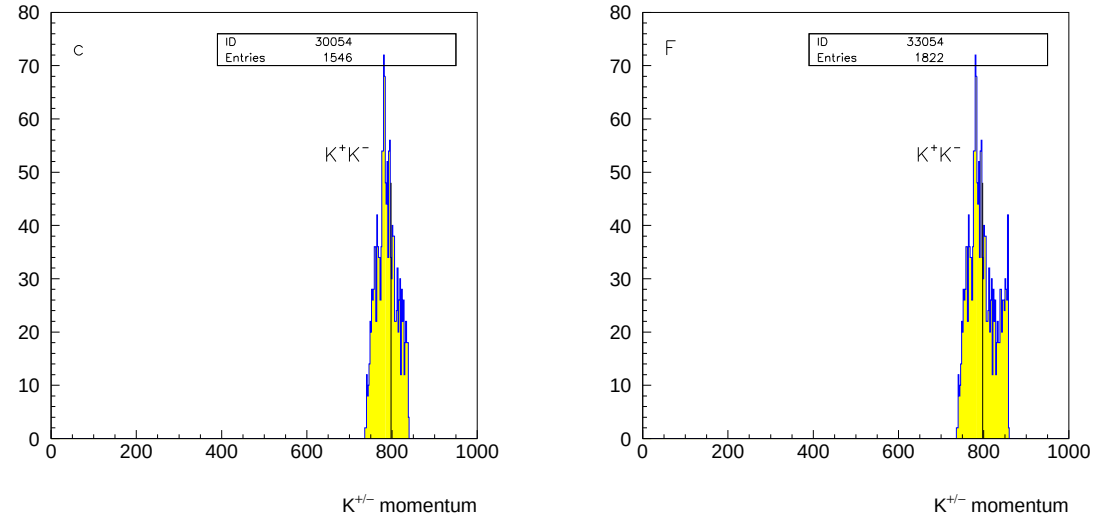

Figure 3.4: Momentum of two prongs. Each event causes two entry. Left region C and right region F (see report [1]).

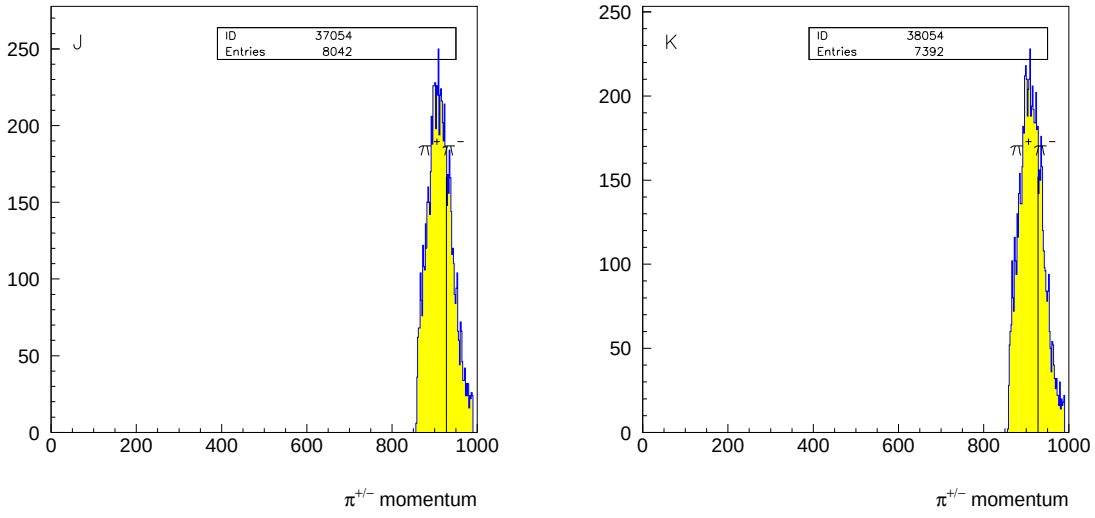

Figure 3.5: Momentum of two prongs. Each event causes on entry. Left region J and right region K (see report [1]).

3.2 $\pi^+\pi^-$ Monte Carlo events

The $\pi^+\pi^-$ Monte Carlo events are produced as usual.

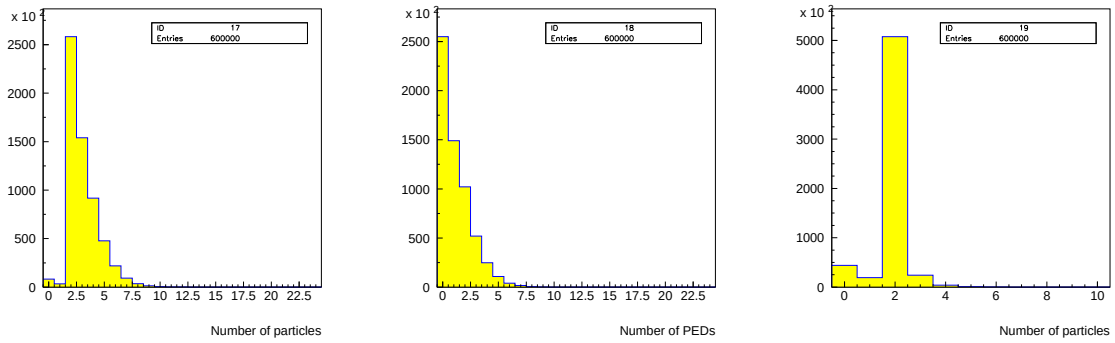

Figure 3.6: The number of particles, PEDs and charged tracks for Monte Carlo events. 600 000 produced Monte Carlo $\pi^+\pi^-$ events are represented in each histogram.

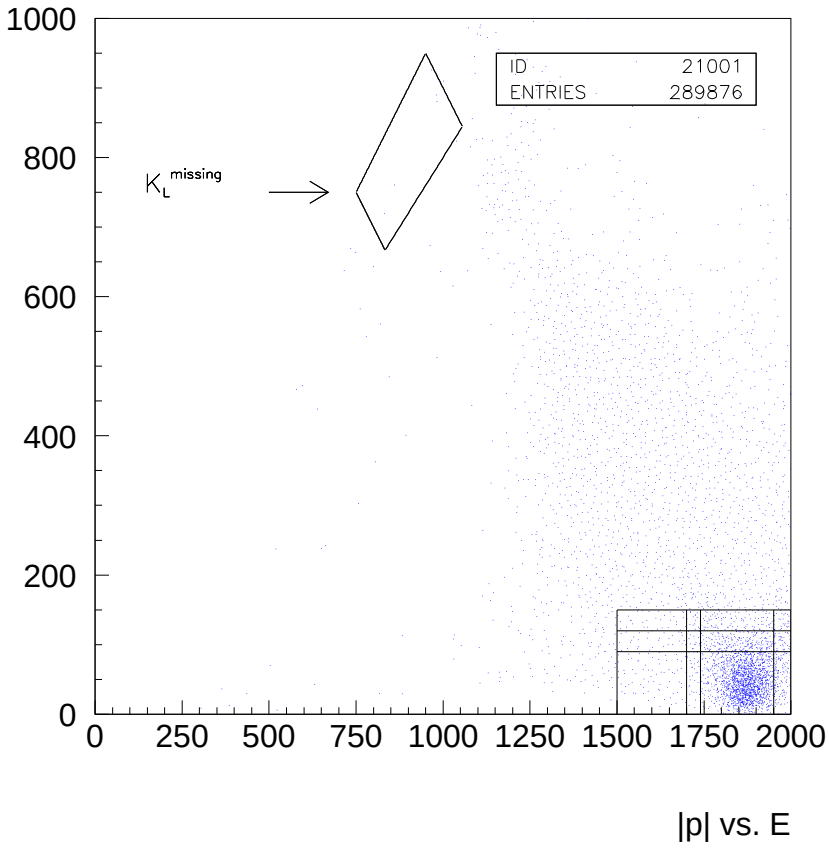

Figure 3.7: $|\vec{p}|$ vs. E. the kinematical regions are defined in report [1].

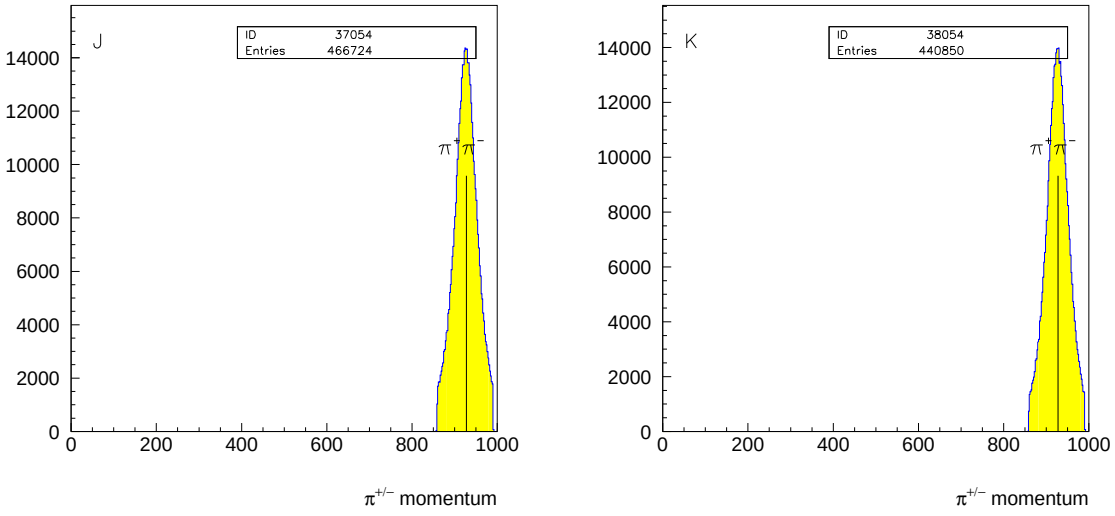

Figure 3.8: Momentum of two prongs. Each event causes two entry per event. Left region G and right region L (see report [1]).

3.3 K^+K^- Monte Carlo events

The K^+K^- Monte Carlo events are produced as usual.

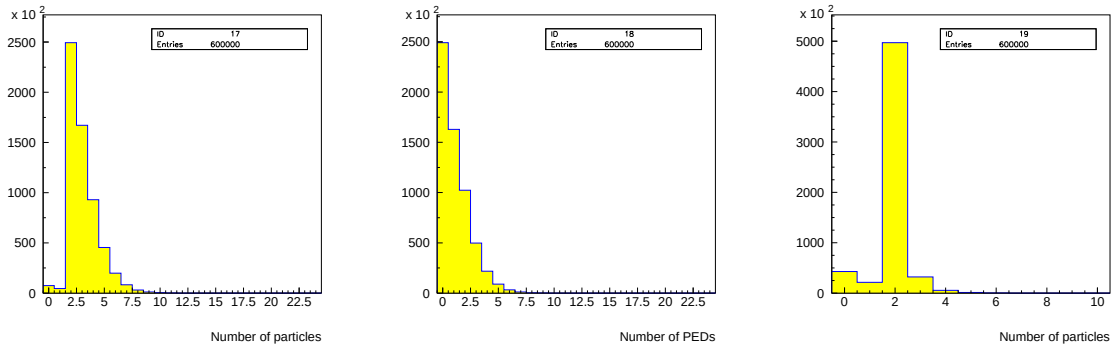

Figure 3.9: The number of particles, PEDs and charged tracks for Monte Carlo events. 600 000 produced Monte Carlo K^+K^- events are represented in each histogram.

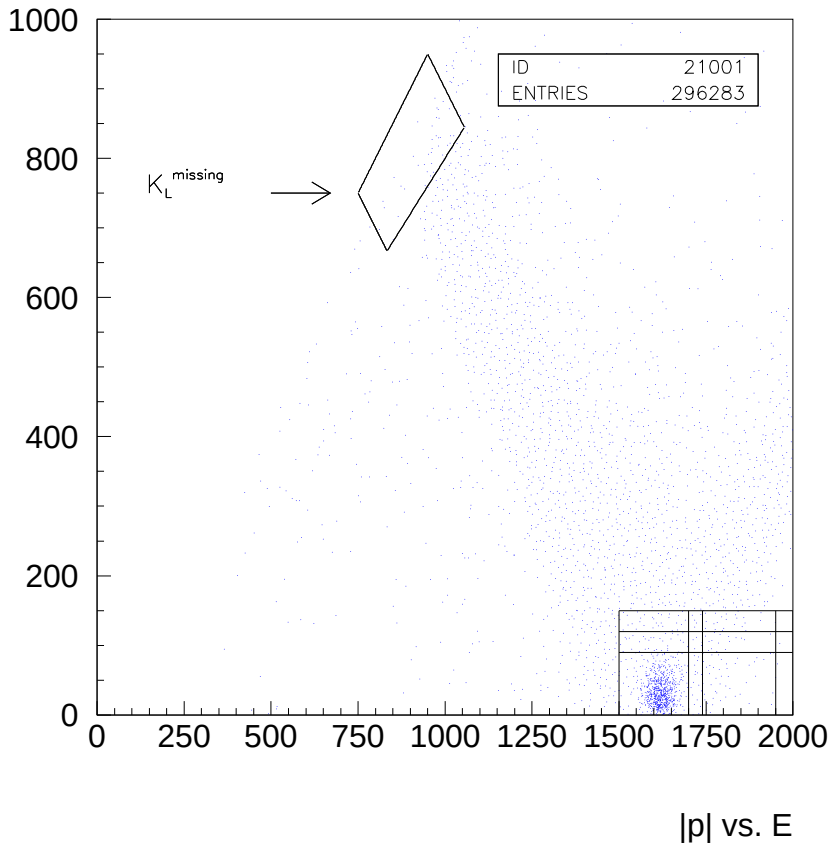

Figure 3.10: $|\vec{p}|$ vs. E. the kinematical regions are defined in report [1].

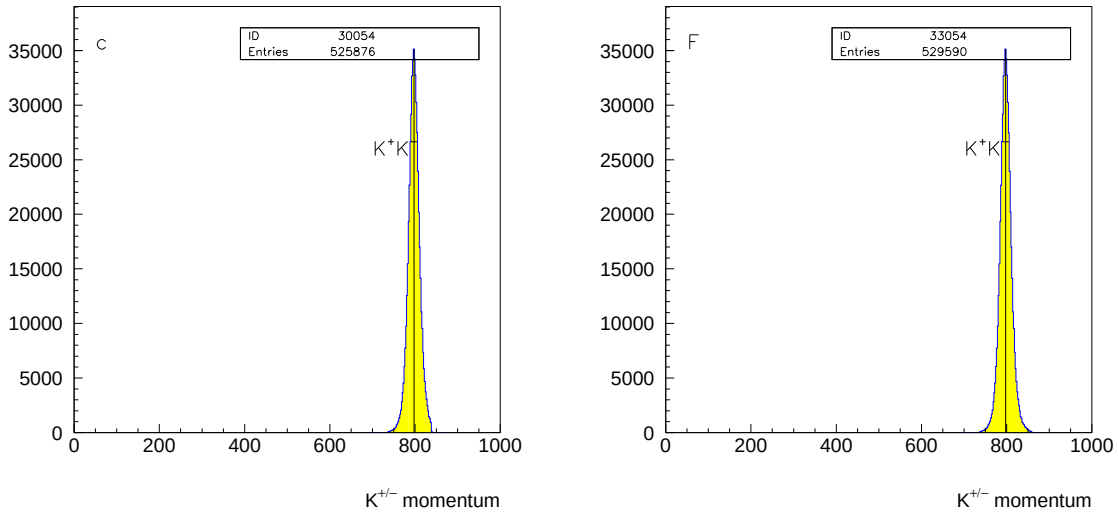

Figure 3.11: Momentum of two prongs. Each event causes two entry per event. Left region C and right region F (see report [1]).

3.4 The Branching Ratios

region	$\#(\pi^+\pi^-)$	#(rec. MC)	$BR(\bar{\mathrm{p}}\mathrm{p} \to \pi^+\pi^-)$
G	3 835	214 319	$(4.140 \pm 0.218) \cdot 10^{-3}$
H	3 545	203 939	$(4.021 \pm 0.212) \cdot 10^{-3}$
I	2 950	180 340	$(3.784 \pm 0.202) \cdot 10^{-3}$
J	4 021	233 362	$(3.986 \pm 0.209) \cdot 10^{-3}$
K	3 696	220 425	$(3.879 \pm 0.204) \cdot 10^{-3}$
L	2 056	192 715	$(3.669 \pm 0.195) \cdot 10^{-3}$

Table 3.1: $\pi^+\pi^-$ branching ratios.

region	$\#(\mathrm{K}^+\mathrm{K}^-)$	#(rec. MC)	$BR(\bar{\mathrm{p}}\mathrm{p} \to \mathrm{K}^+\mathrm{K}^-)$
A	952	225 194	$(9.780 \pm 0.583) \cdot 10^{-4}$
B	880	219 472	$(9.276 \pm 0.559) \cdot 10^{-4}$
C	773	203 251	$(8.792 \pm 0.542) \cdot 10^{-4}$
D	1 149	235 815	$(1.127 \pm 0.065) \cdot 10^{-3}$
E	1 052	228 834	$(1.063 \pm 0.062) \cdot 10^{-3}$
F	911	210 263	$(1.002 \pm 0.060) \cdot 10^{-3}$

Table 3.2: $\mathrm{K}^+\mathrm{K}^-$ branching ratios.

A comparison between real data and Monte Carlo events proves that the regions J and K are the right ones for the determination of the $\pi^+\pi^-$ branching ratio. For $\mathrm{K}^+\mathrm{K}^-$ final state this is region C.

$$BR(\bar{\mathrm{p}}\mathrm{p}(\mathrm{LH}_2) \to \pi^+\pi^-) = (3.93 \pm 0.21) \cdot 10^{-3} \tag{3.1}$$

$$BR(\bar{\mathrm{p}}\mathrm{p}(\mathrm{LH}_2) \to \mathrm{K}^+\mathrm{K}^-) = (8.80 \pm 0.54) \cdot 10^{-4} \tag{3.2}$$

Chapter 4

Summary

Table 4.1 summarizes the results derived in this report. Also the values are compared with previous Crystal Barrel publications and the OBELIX experiment.

$\bar{\mathrm{p}}\mathrm{p} \rightarrow$	target	BR this report
$\pi^0\pi^0$	GH_2	$(1.49 \pm 0.08) \cdot 10^{-3}$
$\pi^0\eta$	GH_2	$(5.52 \pm 0.40) \cdot 10^{-4}$
$\mathrm{K_L K_S}$	GH_2	$(6.83 \pm 0.71) \cdot 10^{-4}$
$\pi^+\pi^-$	GH_2	$(3.93 \pm 0.21) \cdot 10^{-3}$
$\mathrm{K^+K^-}$	GH_2	$(8.80 \pm 0.54) \cdot 10^{-4}$

Table 4.1: Summary of the results.

Bibliography

[1] B. Pick
Technical Report: $\bar{p}p$ annihilation at rest into two-body final states and branching ratios (LH_2)
CB-note 3xx, Bonn 1998

[2] Review of Particle Properties
Phys. Rev. **D54**(1996)